NATURAL RESOURCE MODELING
Volume 12, Number 1, Spring 1999

EDGE PERMEABILITY AND POPULATION PERSISTENCE IN ISOLATED HABITAT PATCHES

R.W. VAN KIRK
Department of Biological Sciences
Idaho State University
Pocatello, ID 83209
E-mail: vankirk@fremontnet.com

M.A. LEWIS
Department of Mathematics
University of Utah
Salt Lake City, Utah 84112
E-mail: mlewis@math.utah.edu

ABSTRACT. Population persistence in isolated habitat fragments is investigated using integrodifference equations. The propensity of individual dispersers encountering the boundary of the patch to emigrate is defined by edge permeability. A dispersal model incorporating movement, settlement and edge permeability defines dispersal success as a function of a disperser's starting location. This dispersal model is used to generate dispersal kernels for integrodifference equation models, analysis of which gives a condition for population persistence in terms of edge permeability, patch size and average dispersal distance. An approximation reduces the spatial problem to a simple nonspatial model that can be easily analyzed.

KEY WORDS. Permeability, integrodifference equations, dispersal, perimeter-to-area ratio, habitat fragmentation.

1. Introduction. Habitat fragmentation affects populations in three ways: 1) by reducing the amount of suitable habitat available, 2) by creating artificially heterogeneous environments and 3) by isolating small populations in remnant habitat patches. Because natural resource managers often have little control over reduction in the amount of suitable habitat available for a particular species, successful management of populations inhabiting fragmented habitats requires an understanding of the effects of heterogeneity and isolation on population persistence. The heterogeneity of a fragmented environment creates an artificial metapopulation situation for species that may not have evolved dispersal strategies appropriate for persistence in such environments (Saunders et al. [1991], Lamberson et al. [1992]). Isolation

subjects small populations to the risks of demographic and environmental stochasticity, genetic deterioration and catastrophic events (Shaffer [1981], Simberloff [1986], Goodman [1987]). Populations in small remnant habitat patches are also negatively impacted by edge effects, which include both alteration of ecological processes within the remnant patch (Lynch and Whigham [1984], Harris [1984], Wilcove [1985], Harris [1988], Brothers and Spingorn [1992], Malcolm [1994]) and negative impacts of interactions with humans at jurisdictional boundaries of designated reserves (Newmark [1985], Shonewald-Cox and Bayless [1986], Wilcove and May [1986], Buechner [1987]). Habitat patch boundaries can directly affect the movement and survival of individual dispersers originating in the interior of the patch, particularly when the boundary delineates changes in human activity or jurisdiction (Oxley et al. [1974], Wegner and Merriam [1979], Lynch and Whigham [1984], Stamps et al. [1987], Duelli et al. [1990], Mader et al. [1990], Reh and Seitz [1990], Newmark [1991]). For example, in an extensive study of grizzly bears, *Ursus actos horribilus*, inhabiting Yellowstone National Park, Craighead [1979] reported that nearly every radio-collared bear that left the protective jurisdiction of the park was killed by humans within a very short amount of time.

The propensity of individual dispersers to cross the boundary of an isolated habitat patch and be removed from the population by hostile conditions outside the patch has been defined as "edge permeability" by Stamps et al. [1987], who utilized simulation modeling to investigate the effects of edge permeability on emigration from isolated habitat patches. The size of the habitat patch at which emigration loss is exactly balanced by reproduction is termed the minimum domain size necessary for population persistence. Minimum domain size problems have often been formulated with reaction-diffusion equations, which assume that reproduction and dispersal occur simultaneously and continuously (Kierstad and Slobodkin [1953], Okubo [1980], Murray [1989], Cantrell and Cosner [1994]). Recently, spatial problems in population ecology and conservation biology have been addressed using integrodifference equations which are discrete-time models capable of separating growth and dispersal phases (Kot and Schaffer [1986], Hardin et al. [1988a], Hardin et al. [1988b], Kot [1989], Hardin et al. [1990], Kot [1992], Neubert et al. [1995], Kot et al. [1996], Veit and Lewis [1996], Van Kirk and Lewis [1997]). The general scalar integrodifference equation has

the form

$$N_{j+1}(\mathbf{x}) = \int_{\Omega} k(\mathbf{x},\mathbf{y}) f(N_j(\mathbf{y});\mathbf{y})\, d\mathbf{y}, \tag{1}$$

where $N_j(\mathbf{x})$ is the population density at a point $\mathbf{x}$ in the habitat patch Ω at the end of the dispersal period in year j, $k(\mathbf{x},\mathbf{y})$ is a nonnegative density function governing the probability of successful dispersal from a point $\mathbf{y}$ in Ω to the point $\mathbf{x}$, $f(N) \equiv g(N)N$ is a nonnegative function, and $g(N)$ is the per capita growth rate. Kot and Schaffer [1986], Hardin et al. [1990] and Van Kirk and Lewis [1997] utilized integrodifference models to investigate population persistence in isolated habitat patches and in heterogeneous environments. However, the models used in these studies assumed passive dispersal, seeds blowing in the wind, for example, and no interaction between individual dispersers and the boundary of the domain.

In this paper we extend the edge permeability concept of Stamps et al. [1987] to an analytical dispersal model that allows conditions at the boundary of an isolated habitat patch to influence emigration and survival of dispersers. We then incorporate this dispersal model into integrodifference models of population growth and dispersal in order to investigate relationships among edge permeability, domain size, emigration loss and population persistence in isolated habitat patches. Section 2 develops a model of active dispersal incorporating movement, settlement and edge permeability and presents results pertaining to edge permeability, patch dimension and emigration. In Section 3 we use integrodifference models constructed around dispersal kernels derived in Section 2 to illustrate how these factors, in turn, affect population persistence.

2. Dispersal, edge permeability and emigration. In general, the dispersal kernel $k(\mathbf{x},\mathbf{y})$ of the integrodifference equation can be derived from a model incorporating movement, mortality, settlement and emigration of individuals during the dispersal period. The probability that an individual starting dispersal at $\mathbf{y}$ survives the dispersal period and settles somewhere in Ω is given by the dispersal success function

$$s(\mathbf{y}) = \int_{\Omega} k(\mathbf{x},\mathbf{y})\, d\mathbf{x}, \tag{2}$$

which is always less than or equal to one. If $s(\mathbf{y})$ is strictly less than one, at least some individuals beginning dispersal at the point $\mathbf{y}$ either die during the dispersal period or settle at a point outside the domain Ω. Since we are interested in the case where Ω is an isolated fragment of habitat, it is assumed that no individuals immigrate into Ω from outside but that dispersers may emigrate from Ω. Average dispersal success is defined by

$$S \equiv \frac{1}{V_\Omega} \int_\Omega s(\mathbf{y})\, d\mathbf{y}, \tag{3}$$

where V_Ω is the size of the patch Ω and $s(\mathbf{y})$ is the dispersal success function defined by Equation (2). The average dispersal rate satisfies the inequality $0 \leq S \leq 1$. We assume throughout this paper that dispersal mortality within Ω is zero so that the only loss of individuals that occurs during the dispersal process is due to emigration from Ω. Under this assumption, emigration is given by $1 - S$.

We now derive a dispersal model that translates assumptions about the movement of individuals into a formulation for the dispersal kernel $k(\mathbf{x}, \mathbf{y})$. These models are discussed in more detail in Neubert et al. [1995] and Van Kirk [1995]. Here we focus on how interactions between the disperser and the edge of the habitat patch determine the shape of the kernel and the emigration rate. Let the dispersal period begin at time $t = 0$ and end at time $t = T$, and consider first a one-dimensional habitat patch given by the interval $[-\hat{L}/2, \hat{L}/2]$. Suppose that dispersers move according to a simple random walk and cease movement to settle at a new location in the domain with rate α per time unit. Then the probability density $u(x, t)$ that an organism beginning dispersal at a point y is still moving at time t is governed by

$$\frac{\partial u}{\partial t} = D \frac{\partial^2 u}{\partial x^2} - \alpha u, \tag{4}$$

with initial condition $u(x, 0) = \delta(x - y)$.

Now suppose that during the random walk the organism takes steps of length Δx during each time interval of duration Δt and that the organism reaches a point on the boundary of the one-dimensional habitat patch at time t. If the random walk were not biased by the boundary, during the subsequent time interval $(t, t + \Delta t]$, the organism

would step back into the interior of the patch with probability 1/2 and would step outside of the patch with probability 1/2. Suppose now that the probability of stepping back inside the interval is still 1/2 but that with the remaining probability 1/2 the disperser either stays at the boundary point or exits the domain, depending on conditions at the boundary. Let the parameter $0 < c < \infty$ represent the rate, per length unit, at which the disperser is enticed to leave the patch. Then the probabilities of stepping back into the patch, remaining stationary at the boundary, and stepping outside of the patch are given by 1/2, $(1 - c\Delta x)/2$ and $c\Delta x/2$, respectively. If it is assumed that conditions outside the boundary are such that dispersers leaving the patch never return, then at the right boundary point $\hat{L}/2$, $u(x,t)$ satisfies

$$u(\hat{L}/2, t + \Delta t) = \frac{1}{2}u(\hat{L}/2 - \Delta x, t) + \frac{1}{2}(1 - c\Delta x)u(\hat{L}/2, t). \tag{5}$$

Expanding each term in a Taylor series and taking the diffusion limit

$$\lim_{\Delta x, \Delta t \to 0} \frac{\Delta x^2}{2\Delta t} = D \tag{6}$$

yields the boundary condition

$$cu(\hat{L}/2, t) + u_x(\hat{L}/2, t) = 0. \tag{7}$$

A similar derivation at the left boundary yields the condition $cu(-\hat{L}/2, t) - u_x(-\hat{L}/2, t) = 0$. The general form of these conditions along the smooth boundary $\partial\Omega$ of a bounded region in $\Re^n$ is given by Robin's boundary condition

$$cu + \frac{\partial u}{\partial \mathbf{n}} = 0 \tag{8}$$

for all $\mathbf{x} \in \partial\Omega$, where $\mathbf{n}$ is the unit outward normal vector to the boundary. As $c \to 0$, dispersers tend to remain inside the patch, and as $c \to \infty$, they tend to leave.

The probability density that the organism is settled at a point x by the end of the dispersal period at time T is given by $\int_0^T \alpha u(x,t)\, dt$. If the duration T of the dispersal period is much longer than the average movement time $1/\alpha$, then to a close approximation, the dispersal period

may be assumed to be infinite in duration, that is, $T \to \infty$. This reflects the biological assumption that, for organisms that have evolved to disperse during a specific season, the inherent movement and settlement rates are such that most dispersers have either settled or emigrated by the end of the dispersal period. Under this assumption, the probability density that a disperser originating at y is settled at x at the end of the dispersal period is given by

$$k(x,y) = \int_0^\infty \alpha u(x,t)\, dt, \tag{9}$$

where the y dependence is conveyed through the initial condition $u(x,0) = \delta(x-y)$.

We now define the dimensionless variables $\tilde{x} = x/\hat{L}$, $\tilde{t} = \alpha t$, $\tilde{c} = \hat{L}c$, $\tilde{u} = \hat{L}u$ and $L = \sqrt{\alpha/D}\hat{L}$. Because the quantity $\sqrt{D/\alpha}$ is the average distance traveled by dispersers before settling in the absence of any boundary effects, the effective domain length L represents the size of the domain relative to the organism's inherent dispersal ability. We also define the dimensionless quantity $p \equiv \tilde{c}/(1+\tilde{c})$, which is the edge permeability of the patch (see Buechner [1987], Stamps et al. [1987]). When $p = 0$, all dispersers that reach the boundary remain in the domain, while at the other extreme, when $p = 1$, all individuals that reach the boundary leave and are removed from the population. Upon dropping the tilde notation on x, t and u for notational simplicity and adopting the subscript notation for partial differentiation, the dispersal process is governed by the dimensionless initial value problem

$$\begin{aligned} u_t(x,t) &= \frac{1}{L^2}u_{xx} - u(x,t), \quad x \in (-1/2, 1/2), \\ u(x,0) &= \delta(x-y), \quad x \in [-1/2, 1/2], \end{aligned} \tag{10}$$

with boundary conditions

$$\begin{aligned} pu(-1/2,t) - (1-p)u_x(-1/2,t) &= 0 \\ pu(1/2,t) + (1-p)u_x(1/2,t) &= 0. \end{aligned} \tag{11}$$

The dimensionless dispersal kernel is given by

$$k(x,y) = \int_0^\infty u(x,t)\, dt, \tag{12}$$

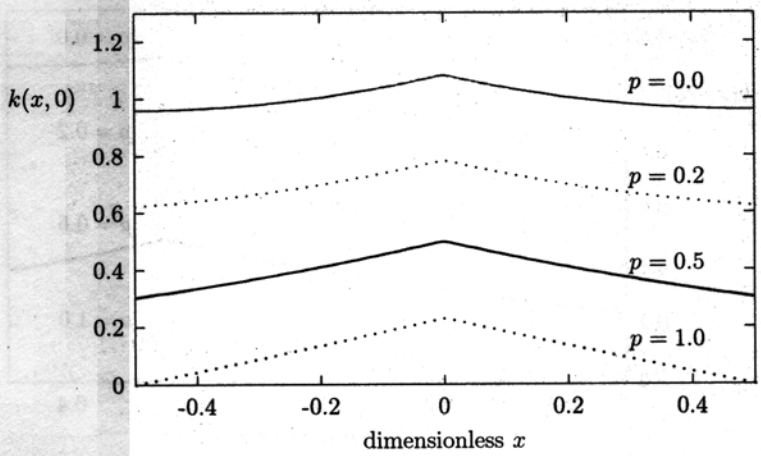

FIGURE 1. Dispersal kernels for effective domain length $L = 1$, disperser point of origin $y = 0$, and various values of the edge permeability p.

which can be derived by solving the initial-boundary value problem directly and integrating. The solution method and resulting Fourier series expressions for $k(x, y)$ are given in Appendix A. Figures 1 and 2 show kernels for different values of p calculated with $L = 1$.

Because dispersers originating in the center of the interval are equally likely to encounter either boundary, all kernels are symmetric around their point of origin when $y = 0$. However, Figure 2 shows that the kernels are not necessarily symmetric around the point of origin when it is moved away from the center of the domain. When edge permeability is high, the kernel has less density on the side of y closest to the boundary. For low edge permeabilities, the boundary acts as a reflector, and there is a correspondingly higher probability that individuals settle between their point of origin and the nearest boundary. Figure 2 also shows that, when $p = 0.5$, the kernel is symmetric around y, even when y is not in the center of the domain. Indeed, when $p = L/(1 + L)$, in this case $p = 1/2$ and $L = 1$, solution of (10) with boundary conditions (11) yields the Laplace kernel

$$k(x, y) = \frac{L}{2} \exp(-L|x - y|), \quad x, y \in [-1/2, 1/2], \tag{13}$$

in which $k(x, y)$ is a function of distance from the disperser's point

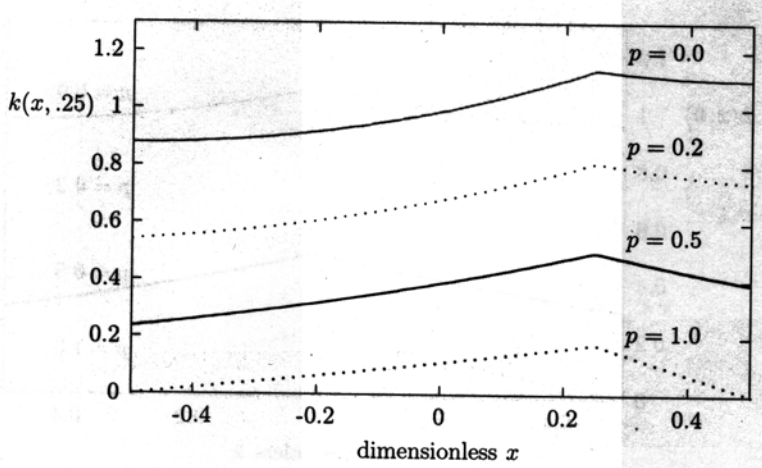

FIGURE 2. Dispersal kernels for effective domain length $L = 1$, disperser point of origin $y = 0.25$, and various values of the edge permeability p.

of origin, regardless of how close to the boundary that point is. The Laplace kernel can be derived from a dispersal process in which individuals move randomly over the infinite real line and settle at a constant rate, Neubert et al. [1995], Van Kirk [1995]. This implies that, when $p = L/(1+L)$, the kernel is identical to the one that would result if the boundary were not there. In this situation, the active dispersal model developed above is equivalent to the passive models considered in Van Kirk and Lewis [1997].

The dispersal success function $s(y) \equiv s(y; p, L) = \int_{-L/2}^{L/2} k(x, y)\, dy$ gives the probability that a disperser originating at the point y in the patch is successfully settled at a new location in the patch at the end of the dispersal period. Figure 3 shows dispersal success functions for $L = 5$ and various values of edge permeability p. The probability that a disperser does not emigrate from the interval is given by the average dispersal success $S \equiv S(p, L) = \int_{-L/2}^{L/2} s(y)\, dy/L$, which is plotted as a function of edge permeability in Figure 4. Not surprisingly, this figure shows that edge permeability has a greater impact on dispersal success in small domains than in large ones, where dispersal success remains fairly high for all but the most permeable edges. Dispersal success is

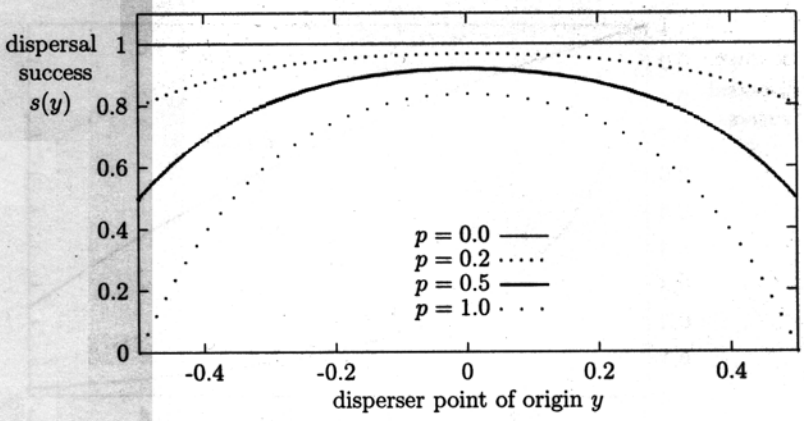

FIGURE 3. Dispersal success functions for effective domain length $L = 5$ and various values of edge permeability p.

given as a function of effective domain length in Figure 5, which shows that increase in dispersal success with domain length is quite abrupt for small permeabilities but is relatively small for highly permeable edges.

To investigate the effects of patch shape on emigration, it is necessary to formulate the dispersal process in two spatial dimensions. Stamps et al. [1987] studied these effects with a simulation model in which organisms moved randomly on a rectangular grid with a constant probability of settling at each step. Two-dimensional diffusive movement on a rectangular domain with a constant settlement rate is the analytical equivalent of their simulation model and the two-dimensional analog to the model developed above. To formulate the two-dimensional model, let (x_1, x_2) be a point in a rectangular domain of dimension $L_1 \times L_2$, and suppose that Robin's boundary conditions given by Equation (8) apply along the boundary of the rectangle. The dimensionless variables are defined by $\tilde{x}_1 = x_1/\sqrt{L_1 L_2}$, $\tilde{x}_2 = x_2/\sqrt{L_1 L_2}$, $\tilde{t} = \alpha t$, $\tilde{c} = \sqrt{L_1 L_2}c$, $\tilde{u} = L_1 L_2 u$, $L \equiv \sqrt{L_1/L_2}$ and $A \equiv L_1 L_2(\alpha/D)$. Edge permeability is again defined as $p = \tilde{c}/(1 + \tilde{c})$. The effective area A is the patch area divided by the square of the average dispersal distance. The perimeter-to-area ratio for the rectangle $[-(L/2), (L/2)] \times [-(1/(2L)), (1/(2L))]$ is given by $R \equiv 2(L + (1/L))$. This nondimensionalization allows

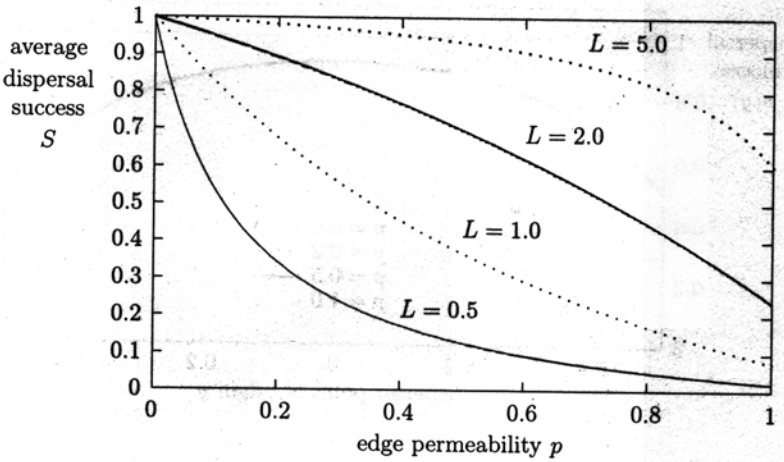

FIGURE 4. Average dispersal success versus edge permeability for various effective domain lengths L.

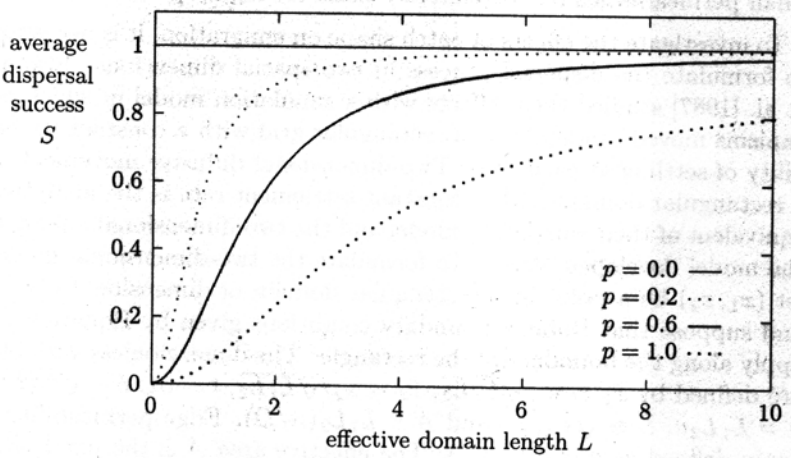

FIGURE 5. Average dispersal success versus effective domain length for various values of the edge permeability p.

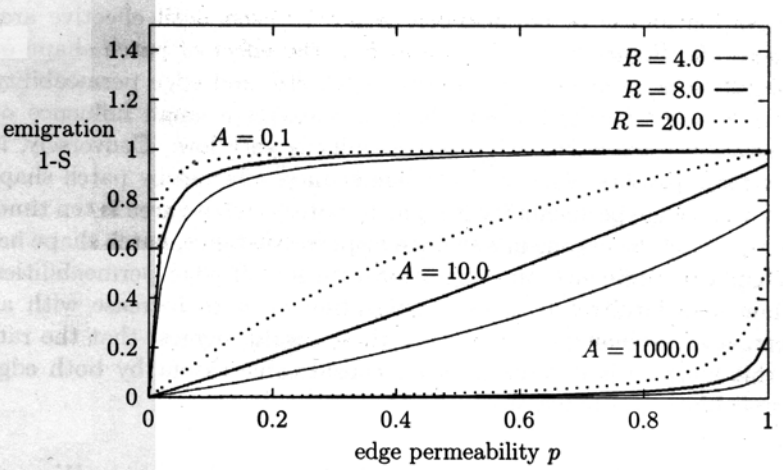

FIGURE 6. Emigration from rectangular habitat patches as a function of edge permeability p and perimeter-to-area ratio R for three different values of effective patch area A.

patch shape R to be varied independently of patch size A. Formulation and solution of the initial-boundary value problem defining this two-dimensional dispersal process is given in Appendix A. Plots of emigration, $1-S(p, R, A)$, versus edge permeability, p, for different perimeter/area ratios, R, and effective areas, A, are shown in Figure 6.

For the smallest patches, the results shown in Figure 6 are nearly identical to those of Stamps et al. [1987], who reported that emigration is a strictly increasing, concave-down function of edge permeability, with higher overall emigration rates when settlement probability is low, perimeter-to-area ratio is high, and patch size is small. However, for intermediate patch sizes, the relationship shown in Figure 6 is nearly linear, and for the largest patches, the relationship is concave up. These results were not reported by Stamps et al., apparently because their simulations were performed only on very small grids. Dispersers in their model moved exactly one grid space each time step, corresponding to a diffusion coefficient $D = 1$. The smallest settlement probability they reported was $\alpha = .05$, which results in an average dispersal distance of $\sqrt{20}$. The largest grid they used had area 40, for an effective area of $40/20 = 2$. Figure 6 suggests that the concave-up relationship between

emigration and edge permeability is not realized until effective area is near 10. Figure 6 also illustrates how the effect of patch shape on emigration is dependent upon both patch size and edge permeability. In very small patches, patch shape size exerts a small influence on emigration rates unless edge permeability is very low. Conversely, in very large patches, emigration is significantly affected by patch shape only when edge permeability is high. In patches whose area is ten times the square of the organism's average dispersal distance, patch shape has a significant influence on emigration rate for all edge permeabilities. While it is intuitive to expect emigration rates to increase with an increase in perimeter-to-area ratio, these results suggest that the rate of this increase is determined to a considerable extent by both edge permeability and patch size.

3. Emigration loss and population persistence. We now utilize integrodifference equations to investigate the effects of edge permeability and domain size on population persistence. Population persistence in Equation (1) requires a balance between the intrinsic growth rate of the population and loss of individuals due to dispersal out of the habitat patch. When the characteristic dispersal distance of the organism is large relative to the size of the isolated patch, dispersers are more likely to settle outside the patch, allowing sink areas to exert a larger negative impact on population persistence than they would if organisms tended to disperse only short distances away from their place of birth. Under the assumptions that (i) the habitat is finite, (ii) during the dispersal period, it is possible for an individual to move from any point in the interior of the habitat patch to any other point in the patch as well as possibly to points outside of the habitat patch, (iii) population growth is finite even at arbitrarily large population densities, (vi) the per capita growth rate $g(N)$ attains its maximum at arbitrarily low densities and decreases with increasing population density and (v) the maximum per capita growth rate is always strictly positive, the persistence of a population modeled by Equation (1) is determined by the magnitude of the largest solution, $\lambda_1 > 0$, of the eigenvalue problem

$$\lambda\phi = \int_\Omega k(\mathbf{x},\mathbf{y})\frac{\partial f}{\partial N}(0;\mathbf{y})\phi(\mathbf{y})\,d\mathbf{y} \tag{14}$$

where $\phi(\mathbf{y})$ is the eigenfunction corresponding to the eigenvalue λ (see

Kot and Schaffer [1986], Hardin et al. [1990], Van Kirk and Lewis [1997]). The parameter λ_1 quantifies the balance between growth and reproduction through the terms $(\partial f/\partial N)$ and $k(\mathbf{x}, \mathbf{y})$, respectively. Using somewhat different approaches, Hardin et al. [1990] and Van Kirk and Lewis [1997] have shown that when $\lambda_1 > 1$, the population persists, and Equation (1) has a positive equilibrium solution describing the density of the population. Furthermore, this solution is unique and globally stable if the growth function $f(N;\cdot)$ models simple, compensatory growth dynamics, i.e., $f(N;\cdot)$ is nondecreasing. The expression $\lambda_1 = 1$ thus implicitly defines the relationship between various biological parameters at the bifurcation point. For one-dimensional domains, solution of this equation in terms of the effective domain length parameter L defines the minimum domain size L_m necessary for persistence of the population.

Consider a population modeled by Equation (1) on the one-dimensional domain $[-1/2, 1/2]$, with dispersal process governed by the dimensionless Equations (10)–(12). Suppose that the growth function $f(N)$ does not depend explicitly on y. For notational simplicity, let $r = (\partial f/\partial N)(0)$, see Equation (14), and let the assumptions (i)–(v) of Section 2 hold. Then λ_1 is a solution to the eigenvalue problem

$$\lambda\phi = \int_{-1/2}^{1/2} k(x,y) r \phi(y)\, dy. \tag{15}$$

To find an explicit expression for λ_1, it is useful to express Equation (15) in an alternate form. Because the kernel is defined in terms of the differential equation (10), it can be shown (see Van Kirk [1995]) that Equation (15) is equivalent to the differential equation

$$\phi_{xx} = -L^2\left(\frac{r}{\lambda} - 1\right)\phi(x), \tag{16}$$

with boundary conditions

$$\begin{aligned} p\phi(-1/2) - (1-p)\phi_x(-1/2) &= 0 \\ p\phi(1/2) + (1-p)\phi_x(1/2) &= 0. \end{aligned} \tag{17}$$

Solution of this equation yields the relationship

$$p\cos\left(\frac{L}{2}\sqrt{\frac{r}{\lambda} - 1}\right) - (1-p)L\sqrt{\frac{r}{\lambda} - 1}\sin\left(\frac{L}{2}\sqrt{\frac{r}{\lambda} - 1}\right) = 0. \tag{18}$$

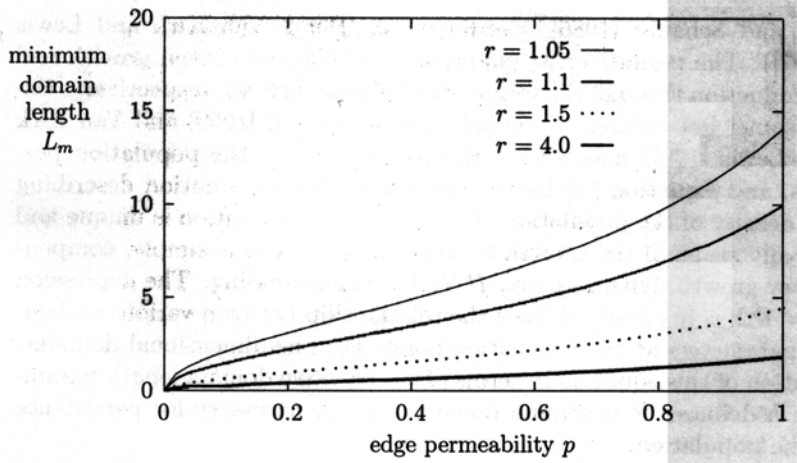

FIGURE 7. Minimum domain size L_m versus edge permeability for different values of intrinsic growth rate r.

At the point where reproduction exactly balances emigration loss, $\lambda = \lambda_1 = 1$ and Equation (18) can be rearranged to obtain

$$(19) \qquad (1-p)L_m\sqrt{r-1} = p\cot\frac{L_m\sqrt{r-1}}{2}.$$

This relationship defines minimum domain size as a function of p and r as shown in Figure 7. It is interesting to note that Equation (19) is similar to expressions for minimum domain size that can be obtained from reaction-diffusion equations describing continuous growth and dispersal on finite domains with Robin's boundary conditions (see Okubo [1980], Murray [1989], Cantrell and Cosner [1994]).

Although an analogous two-dimensional model does not generally yield a closed-form expression for minimum domain size, the two-dimensional model of Section 3 on a square domain does allow a convenient expression for the minimum domain size. Analysis similar to that presented above yields a relationship identical to Equation (19) with L replaced by $\sqrt{A/2}$, where A is the effective area defined in Section 3.

Figure 7 shows how edge permeability has a large effect on minimum domain size only for low intrinsic growth rates. While this model

is somewhat idealized, these low intrinsic growth rates are typical of those of large, long-lived organisms such as the grizzly bear (Knight and Eberhard [1985]) and northern spotted owl, *Strix occidentalis caurina* (Lamberson et al.[1992]), suggesting that these species are more susceptible to the effects of isolation than more fecund species. Because domain length L has already been scaled relative to the organism's average dispersal distance, these results imply that large organisms require large habitat patches for persistence not only because they have large characteristic dispersal distances but also because they have inherently low reproductive rates. More realistic models of reproduction and dispersal in these types of organisms would incorporate age structure and account for the observation that not all individuals disperse during every dispersal period.

We conclude with a more general result on the relationships among dispersal success, intrinsic growth rate and population persistence in isolated patches (see Van Kirk and Lewis [1997]). In applied management situations, specific values for parameters such as edge permeability and effective domain size are unlikely to be readily available. However, data collected from mark-recapture experiments and other census activities may provide estimates of dispersal success and reproductive rates. The following result provides a simple method to evaluate persistence of a population with knowledge of only these two parameters.

Let $N_*(\mathbf{x})$ denote the nonnegative equilibrium solution to Equation (1) in the case that f does not depend explicitly on $\mathbf{y}$. Then

$$N_*(\mathbf{x}) = \int_\Omega k(\mathbf{x},\mathbf{y}) f(N_*(\mathbf{y}))\, d\mathbf{y}. \tag{20}$$

Now let

$$\overline{N} \equiv \frac{1}{V_\Omega} N_*(\mathbf{x})\, d\mathbf{x} \tag{21}$$

denote the spatial average of the equilibrium solution. The size of the equilibrium population is thus given by $V_\Omega \overline{N}$. If the derivative $f'(N)$ of the growth function is continuous, then, for each $\mathbf{y} \in \Omega$, $f(N_*(\mathbf{y}))$ has a Taylor expansion of the form

$$f(N_*(\mathbf{y})) = f(\overline{N}) + f'(\hat{N}(\mathbf{y}))(N_*(\mathbf{y}) - \overline{N}) \tag{22}$$

where $\hat{N}(\mathbf{y})$ lies between $\overline{N}$ and $N_*(y)$. Substituting this into Equation (20) yields

$$N_*(x) = f(\overline{N}) \int_\Omega k(\mathbf{x},\mathbf{y})\, d\mathbf{y} + \int_\Omega k(\mathbf{x},\mathbf{y}) f'(\hat{N}(\mathbf{y}))(N_*(\mathbf{y}) - \overline{N})\, d\mathbf{y}. \tag{23}$$

Integrating Equation (20) with respect to $\mathbf{x}$, dividing by V_Ω, using the definition of $\overline{N}$, and recalling that $S = (1/V_\Omega) \int_\Omega \int_\Omega k(\mathbf{x},\mathbf{y})\, d\mathbf{x}\, d\mathbf{y}$ yields

$$\overline{N} = Sf(\overline{N}) + \frac{1}{V_\Omega} \int_\Omega s(\mathbf{y}) f'(\hat{N}(\mathbf{y}))(N_*(\mathbf{y}) - \overline{N})\, d\mathbf{y}. \tag{24}$$

Thus a first-order approximation to $\overline{N}$ is the solution to the algebraic equation

$$\overline{N}_{\text{appr}} = Sf(\overline{N}_{\text{appr}}), \tag{25}$$

which defines an approximate relationship among dispersal success S, population growth $f(N)$ and the size of the equilibrium population. When dispersal success and fecundity are both sufficiently high that the solution $\overline{N}_{\text{appr}}$ exists and is positive, conditions necessary for persistence are met. The quantity $V_\Omega \overline{N}_{\text{appr}}$ is an estimate of the equilibrium population size, which, in turn, determines the susceptibility of the population to the effects of stochasticity and genetic deterioration.

To illustrate the utility of Equation (25), consider an integrodifference equation utilizing the Beverton and Holt [1957] growth function

$$f(N) = \frac{rN}{1 + [(r-1)N/K]}, \tag{26}$$

which models compensatory growth. The parameter r is the per capita intrinsic growth rate as defined above. After normalizing the carrying capacity K to unity, Equation (25) for this problem becomes

$$\overline{N}_{\text{appr}} = \frac{Sr\overline{N}_{\text{appr}}}{1 + (r-1)\overline{N}_{\text{appr}}}, \tag{27}$$

with solution

$$\overline{N}_{\text{appr}} = \frac{Sr - 1}{r - 1}. \tag{28}$$

In this case the population persists when $S > 1/r$, and equilibrium population size increases linearly with dispersal success S at a rate proportional to $r/(r-1)$. Figure 8 shows true and approximate equilibrium population size as a function of dispersal success S and intrinsic growth rate r. The true solution was calculated from the full integrodifference model utilizing the Beverton-Holt growth function. The kernel utilized in this example is one defined by Equations (10)–(12) with p and L varied in such a way that dispersal success S changes, but the relationship $L = p/(1-p)$ holds throughout the range of parameter values. The approximate solution is given by Equation (28). The linear relationship between population size and dispersal success predicted by the approximation is immediately evident in the bifurcation diagram. Discrepancy between the true and approximate solution at higher values of S may be due to numerical instability introduced by the large effective domain size values L that must be used to obtain the higher values of S. Because $S = 1$ is achieved in the true solution only as L becomes infinitely large, the calculations were truncated at $S = 0.9$ ($L = 10.0$). Figure 8 also illustrates again the relatively high degree of sensitivity of population persistence to changes in dispersal success when the intrinsic population growth rate is low.

4. Discussion. Edge permeability provides a conceptual and quantitative link between edge effects and dispersal success in isolated habitat patches by allowing the movement behavior and survival of dispersers originating inside an isolated habitat patch to be affected by conditions at the boundary. The results of Section 3 show how loss of dispersers due to emigration from the patch increases with increasing edge permeability, decreasing patch size, and increasing perimeter-to-edge ratio. The effects of edge permeability on emigration increase in smaller patches and those with higher edge-to-area ratios, as predicted by the model of Stamps et al. [1987]. However, our results emphasize two additional observations.

First, the influence of patch shape on emigration is affected by both edge permeability and patch size. Figure 6 shows that emigration is

mention grizzly dispersal at all, see Mattson and Reid [1991] for an extensive bibliography, but Blanchard and Knight [1991] estimated an average dispersal distance of 70 km. This results in an effective are of $A = 1.8$ for the park. Figure 6 suggests that this effective area is relatively small and falls within the parameter range for which emigration rates are high for all but the most impermeable edges. These model predictions are consistent with the observations of Craighead [1979], who reported that bears freely crossed park boundaries but were frequently killed upon exiting the park, and of Mattson and Reid [1991], who reported that 81 percent of all known Yellowstone grizzly mortalities between 1975–1988 were caused by conflicts with humans, most of these occurring outside of the park boundary.

Second, the impacts of patch size and edge permeability on population persistence are proportionally greater to species with inherently low fecundity. This result is particularly significant because large organisms such as grizzly bears, which generally have low fecundities, are frequently the objects of natural resource management plans designed to provide habitat patches large enough to maintain population viability. Our results suggest that large organisms need large habitat patches not only because they have large territory requirements and disperse long distances, but perhaps just as importantly, because they have low reproductive rates. On the time scale of the long life spans that typify these large organisms, fecundity is not sufficient to outweigh the annual loss of dispersers that occurs when populations are restricted to small, isolated habitat fragments surrounded by inhospitable terrain.

Although edge permeability in our model is defined in terms of the theoretical boundary condition parameter c, our dispersal model provides empirical researchers with a method for estimating edge permeability and thus testing hypotheses about its effects on emigration from isolated habitat patches. In one dimension, edge permeability can be estimated from knowledge of effective domain length L and dispersal success $s(y)$ for disperser originated near the boundary of the domain. Effective domain length is given by $L = \hat{L}/\bar{d}$, where $\hat{L}$ is actual domain length of the isolated habitat patch and $\bar{d}$ is the arithmetic mean of dispersal distances in the absence of boundary effects ($\bar{d} = \sqrt{D/\alpha}$ in the model derived in Section 3). Dispersal distance is the straight-line distance between a disperser's point of origin and its point of settlement at the end of the dispersal period. This quantity can be measured by

marking the location of individual dispersers at the beginning of the dispersal period and recording their locations at the end of the dispersal period. These measurements should be made in a habitat patch that is sufficiently large that observed dispersers do not encounter the boundary of the patch. Once L is known, the Fourier series forms of the dispersal kernel, Equation (35) ($p = 0$), Equation (36) ($p = 1$) and Equation (38) ($0 < p < 1$), can be integrated with respect to x to obtain expressions for the dispersal success function $s(y)$ at various values of edge permeability p. The integrals of Equations (35), (36) and (38) predict the probability of dispersal success as a function of disperser point of origin and generate graphs such as those shown in Figure 3. Measurement of dispersal success rates for dispersers originating at points near the edge of the domain can then be used to estimate p from the relationships described graphically in Figure 3. Once an estimate of p is obtained, Equations (35), (36) and (38) can be integrated with respect to both x and y to predict the spatially averaged dispersal success rate S. Relationships among S, L and p are illustrated in Figures 4 and 5. If the average dispersal success S can be readily measured, comparison of the actual S with that predicted by the estimate of edge permeability provide a test of the model's applicability.

While this procedure provides a feasible method for estimating edge permeability for small organisms where dispersal distances are small and the fate of individual dispersers can be readily observed, empiricists working with large organisms may not be able to observe dispersal distances and fates of individual dispersers. For example, Blanchard and Knight [1991] were able to quantify only two instances of grizzly dispersal. Furthermore, Doak et al. [1992] reported that, even among studies devoted specifically to dispersal in a variety of organisms, very few reported the spatial scale of habitat patches relative to characteristic dispersal distances. However, the approximation given by Equation (25) provides a simple, algebraic method for quantifying population persistence even when information on dispersal distance and edge permeability is not available or easily obtained. The only spatial information required by the approximation is average dispersal success, S, which is much more easily measured using standard population census procedures than dispersal distance, edge permeability, or other dispersal-specific parameters. Conditions necessary for population persistence are met when Equation (25) has a positive solution. Thus, the

approximation provides a way to quantify the sensitivity of population persistence to changes in dispersal success and intrinsic growth rates regardless of the mechanisms by which edge permeability and patch shape affect dispersal success.

5. Acknowledgments. This research was supported in part by a University of Utah Graduate Research Fellowship (RVK) and by grants from the National Science Foundation, DMS-94-57816, and the Alfred P. Sloan Foundation (MAL).

Appendix

A. To formulate the dispersal kernel defined by Equations (10)–(12), we first note that the operator

$$\mathcal{L} = \frac{1}{L^2}\frac{\partial^2}{\partial x^2} \tag{29}$$

with boundary conditions (11) is a self-adjoint operator of Sturm-Liouville type and has an orthogonal set of eigenfunctions $\{\phi_n(x)\}_{n=1}^{\infty}$ (Birkhoff and Rota [1978]), where

$$\phi_n(x) = A\cos(b\lambda_n x) + B\sin(b\lambda_n x).$$

The solution $u(x,t)$ to Equation (10) thus has the form

$$u(x,t) = \sum_{n=1}^{\infty} \hat{u}_n(t)\frac{1}{\|\phi_n\|_2^2}\phi_n(x), \tag{30}$$

where

$$\|\phi_n\|_2^2 = \int_{-1/2}^{1/2} \phi_n^2(x)\,dx \tag{31}$$

and

$$\hat{u}_n(t) = \int_{-1/2}^{1/2} u(x,t)\phi_n(x)\,dx. \tag{32}$$

Applying the transform defined by Equation (32) and using the properties of $\phi_n(x)$, the solution is found to be

$$u(x,t) = \sum_{n=1}^{\infty} \frac{1}{\|\phi_n\|_2^2} \exp[-(\lambda_n^2 + 1)t]\phi_n(x)\phi_n(y), \tag{33}$$

where the y dependence is derived from the initial condition $u(x,0) = \delta(x-y)$ of Equation (10). The kernel is given by $\int_0^\infty u(x,t)\,dt$, which may be computed by integrating term-wise inside the summation, since the series converges absolutely for $0 < t < \infty$.

Application of the boundary conditions requires consideration of three different cases according to the value of p.

Case 1. When $p = 0$, the boundary conditions reduce to

$$\phi_n'(\pm 1/2) = 0,$$

which yields the homogeneous system

$$\begin{aligned} AL\lambda_n \sin\frac{L\lambda_n}{2} + BL\lambda_n \cos\frac{L\lambda_n}{2} &= 0 \\ -AL\lambda_n \sin\frac{L\lambda_n}{2} + BL\lambda_n \cos\frac{L\lambda_n}{2} &= 0. \end{aligned} \tag{34}$$

Solution of this system yields the kernel

$$\begin{aligned} k(x,y) = 1 &+ \sum_{n=1}^{\infty} \frac{2L^2}{4n^2\pi^2 + L^2} \cos 2n\pi x \cos 2n\pi y \\ &+ \frac{2L^2}{(2n-1)^2\pi^2 + L^2} \sin(2n-1)\pi x \sin(2n-1)\pi y. \end{aligned} \tag{35}$$

Case 2. When $p = 1$, the boundary conditions reduce to $\phi_n(\pm 1/2) = 0$, and computation similar to that of the first case yields

$$\begin{aligned} k(x,y) = \sum_{n=1}^{\infty} &\frac{2L^2}{(2n-1)^2\pi^2 + L^2} \cos(2n-1)\pi x \cos(2n-1)\pi y \\ &+ \frac{2L^2}{4n^2\pi^2 + L^2} \sin 2n\pi x \sin 2n\pi y. \end{aligned} \tag{36}$$

Case 3. When $0 < p < 1$, the boundary conditions give the system

$$pA\cos\frac{L\lambda_n}{2} - pB\sin\frac{L\lambda_n}{2} - (1-p)AL\lambda_n \times \sin\frac{L\lambda_n}{2} - (1-p)BL\lambda_n\cos\frac{L\lambda_n}{2} = 0,$$

$$pA\cos\frac{L\lambda_n}{2} + pB\sin\frac{\lambda_n}{2} - (1-p)AL\lambda_n \times \sin\frac{L\lambda_n}{2} + (1-p)BL\lambda_n\cos\frac{L\lambda_n}{2}. \tag{37}$$

In this case the kernel is given by

$$k(x,y) = \sum_{n=1}^{\infty}\left[\frac{2L\lambda_n}{L\lambda_n + \sin L\lambda_n}\right]\frac{1}{\lambda_n^2+1}\cos L\lambda_n x\cos L\lambda_n y + \left[\frac{2L\lambda_{n^*}}{L\lambda_{n^*} - \sin L\lambda_{n^*}}\right]\frac{1}{\lambda_{n^*}^2+1}\sin L\lambda_{n^*}x\sin L\lambda_{n^*}y, \tag{38}$$

where λ_n is the positive solution to the equation

$$\lambda_n = \frac{p}{(1-p)L}\cot\frac{L\lambda_n}{2}, \quad n = 1,2,\ldots \tag{39}$$

on the nth branch of the cotangent function and λ_{n^*} is the positive solution to the equation

$$\lambda_{n^*} = -\frac{p}{(1-p)L}\tan\frac{L\lambda_{n^*}}{2}, \quad n = 1,2,\ldots \tag{40}$$

on the nth branch of the tangent function.

In two spatial dimensions, the nondimensionalized dispersal process is given by

$$\begin{gathered} u_t(x_1,x_2;t) = \frac{1}{A}\nabla^2 u(x_1,x_2;t) - u(x_1,x_2;t), \\ -L/2 < x_1 < L/2, -1/2L < x_2 < 1/2L, \\ u(x_1,x_2;0) = \delta(\mathbf{x}-\mathbf{y}), \\ pu(-L/2,x_2;t) - (1-p)u_{x1}(-L/2,x_2;t) = 0, \\ pu(L/2,x_2;t) + (1-p)u_{x1}(L/2,x_2;t) = 0, \\ pu(x_1,-1/2L;t) - (1-p)u_{x2}(x_1,-1/2L;t) = 0, \\ pu(x_1,1/2L;t) + (1-p)u_{x2}(x_1,1/2L;t) = 0, \\ k(\mathbf{x},\mathbf{y}) = \int_0^{\infty} u(\mathbf{x};t)\,dt, \end{gathered} \tag{41}$$

where $\mathbf{x} = (x_1, x_2)$. Because the problem is formulated on a rectangular domain with constant diffusion coefficient, the x_1 and x_2 variables may be separated, and thus the two-dimensional eigenfunctions consist of the product of the one-dimensional eigenfunctions that individually satisfy the separated, one-dimensional subsystem in the x_1 and x_2 directions. The kernel has the general form

$$k(\mathbf{x}, \mathbf{y}) = \sum_{n=1}^{\infty} \sum_{m=1}^{\infty} \frac{\Phi_{nm}(\mathbf{x}) \Phi_{nm}(\mathbf{y})}{\|\Phi_{nm}\|_2^2 (a_n^2 + b_m^2 + 1)}, \tag{42}$$

where

$$\begin{aligned} \Phi_{nm}(\mathbf{x}) &= \phi_{1n}(x_1)\phi_{2m}(x_2), \\ \phi''_{1n}(x_1) &= -A a_n^2 \phi_{1n}(x_1), \\ \phi''_{2m}(x_2) &= -A b_m^2 \phi_{2m}(x_2), \end{aligned} \tag{43}$$

$\phi_{1n}(x_1)$ satisfies the boundary conditions at $x_1 = -L/2$ and $x_1 = L/2$ and $\phi_{2m}(x_2)$ satisfies the boundary conditions at $x_2 = -1/2L$ and $x_2 = 1/2L$. Using the general form (42) and the specific results of the one-dimensional analysis presented above, the kernel is found to have the following forms:

p = 0:

$$\begin{aligned} k(\mathbf{x}, \mathbf{y}) &= L + 1/L \\ &+ \sum_{n=1,m=1}^{\infty} \frac{4\sqrt{A}L}{4n^2\pi^2 + 4m^2\pi^2 L^2 + \sqrt{A}L} \\ &\times \cos(2n\pi x_1/L) \cos(2n\pi y_1/L) \cos(2m\pi L x_2) \cos(2m\pi L y_2) \\ &+ \sum_{n,m=1}^{\infty} \frac{4\sqrt{A}L}{4n^2\pi^2 + 4m^2\pi^2 L^2 + \sqrt{A}L} \sin[(2n-1)\pi x_1/L] \\ &\times \sin[(2n-1)\pi y_1/L] \sin[(2m-1)\pi L x_2] \sin[(2m-1)\pi L y_2]. \end{aligned} \tag{44}$$

p = 1:

$$
\begin{aligned}
&k(\mathbf{x},\mathbf{y}) \\
&= \sum_{n,m=1}^{\infty} \frac{4\sqrt{A}L}{4n^2\pi^2 + 4m^2\pi^2L^2 + \sqrt{A}L} \\
&\times \cos[(2n-1)\pi x_1/L]\cos[(2n-1)\pi y_1/L] \\
&\times \cos[(2m-1)\pi L x_2]\cos[(2m-1)\pi L y_2] \\
&+ \sum_{n,m=1}^{\infty} \frac{4\sqrt{A}L}{4n^2\pi^2 + 4m^2\pi^2L^2 + \sqrt{A}L} \\
&\times \sin(2n\pi x_1/L)\sin(2n\pi y_1/L)\sin(2m\pi L x_2)\sin(2m\pi L y_2).
\end{aligned} \tag{45}
$$

0 < p < 1:

$$
\begin{aligned}
&k(\mathbf{x},\mathbf{y}) \\
&= \sum_{n,m=1}^{\infty} \left[\frac{2\sqrt{A}a_n}{L\sqrt{A}a_n + \sin\sqrt{A}La_n}\right]\left[\frac{2\sqrt{A}Lb_m}{\sqrt{A}b_m + L\sin\sqrt{A}b_m/L}\right] \\
&\times \left[\frac{\cos\sqrt{A}a_nx_1\cos\sqrt{A}a_ny_1\cos\sqrt{A}b_mx_2\cos\sqrt{A}b_my_2}{a_n^2+b_m^2+1}\right. \\
&+ \sum_{n,m=1}^{\infty} \left[\frac{2\sqrt{A}c_n}{L\sqrt{A}c_n - \sin\sqrt{A}La_n}\right]\left[\frac{2\sqrt{A}Ld_m}{\sqrt{A}d_m - L\sin\sqrt{A}d_m/L}\right] \\
&\times \left.\frac{\sin\sqrt{A}c_nx_1\sin\sqrt{A}c_ny_1\sin\sqrt{A}d_mx_2\sin\sqrt{A}d_my_2}{c_n^2+d_m^2+1}\right],
\end{aligned} \tag{46}
$$

where a_n is the positive solution to the equation

$$
a_n = \frac{p}{(1-p)\sqrt{A}}\cot\frac{\sqrt{A}La_n}{2} \tag{47}
$$

on the nth branch of the cotangent function, b_m is the positive solution to the equation

$$
b_m = \frac{p}{(1-p)\sqrt{A}}\cot\frac{\sqrt{A}Lb_m}{2L} \tag{48}
$$

on the mth branch of the cotangent function, c_n is the positive solution to the equation

$$c_n = -\frac{p}{(1-p)\sqrt{A}} \tan \frac{\sqrt{A} L c_n}{2} \tag{49}$$

on the nth branch of the tangent function, and d_m is the positive solution to the equation

$$d_m = -\frac{p}{(1-p)\sqrt{A}} \tan \frac{\sqrt{A} d_m}{2L} \tag{50}$$

on the mth branch of the tangent function.

REFERENCES

R.J.H Beverton and S.J. Holt [1957], *On the Dynamics of Exploited Fish Populations*, Fisheries Investigations **19**, Ministry of Agriculture, Fisheries and Food, London.

G. Birkhoff and G.-C. Rota [1978], *Ordinary Differential Equations*, Wiley, New York.

B.M. Blanchard and R.R. Knight [1991], *Movements of Yellowstone Grizzly Bears*, Biological Conservation **58**, 41–67.

T.S. Brothers and A. Spingorn [1992], *Forest Fragmentation and Alien Plant Invasion of Central Indiana Old Growth Forests*, Conservation Biology **6**, 91–100.

M. Buechner [1987], *Conservation in Insular Parks: Simulation Models of Factors Affecting the Movement of Animals across Park Boundaries*, Biological Conservation **41**, 57–76.

R.S. Cantrell and C. Cosner [1994], *Insular Biogeographic Theory and Diffusion Models in Population Dynamics*, Theoret. Pop. Biology **45**, 177–207.

F.C. Craighead, Jr. [1979], *Track of the Grizzly*, Sierra Club Books, San Francisco.

D.F. Doak, P.C. Marino and P.M. Kareiva [1992], *Spatial Scale Mediates the Influence of Habitat Fragmentation*, Theoret. Pop. Biology **41**, 315–336.

E. Doedel, X. Wang and T. Fairgrieve [1994], *Software for Continuation and Bifurcation Problems in Ordinary Differential Equations*, Technical Report, California Institute of Technology, Pasadena, CA.

P. Duelli, M. Studer, I. Marchand and S. Jakob [1990], *Population Movements of Arthropods between Natural and Cultivated Areas*, Biological Conservation **54**, 193–207.

D. Goodman [1987], *The Demography of Chance Extinction* in *Viable Populations for Conservation* (M.E. Soulé, ed.), Cambridge University Press, Cambridge, MA, 11–34.

D.P. Hardin, P. Takac and G.F. Webb [1988a], *Asymptotic Properties of a Continuous-Space Discrete-Time Population Model in a Random Environment*, J. Math. Biology **26**, 361–374.

D.P. Hardin, P. Takac and G.F. Webb [1988b], *A Comparison of Dispersal Strategies for Survival of Spatially Heterogeneous Populations*, SIAM J. Appl. Math. **48**, 1396–1423.

D.P. Hardin, P. Takac and G.F. Webb [1990], *Dispersion Population Models Discrete in Time and Continuous in Space*, J. Math. Biology **28**, 1–20.

L. Harris [1984], *The Fragmented Forest: Island Biogeography Theory and the Preservation of Biotic Diversity*, University of Chicago Press, Chicago.

L.D. Harris [1988], *Edge Effects and Conservation of Biotic Diversity*, Conservation Biology **2**, 330–332.

H. Kierstad and L.B. Slobodkin [1953], *The Size of Water Masses Containing Plankton Blooms*, J. Marine Research **12**, 141–147.

R. Knight and L.L. Eberhardt [1985], *Population Dynamics of Yellowstone Grizzly Bears*, Ecology **66**, 323–334.

M. Kot [1989], *Diffusion-Driven Period-Doubling Bifurcations*, BioSystems **22**, 279–287.

M. Kot [1992], *Discrete-Time Travelling Waves: Ecological Examples*, J. Math. Biology **30**, 413–436.

M. Kot and W. Schaffer [1986], *Discrete-Time Growth-Dispersal Models*, Mathematical Biosciences **80**, 109–136.

M. Kot, M.A. Lewis and P. van den Driessche [1996], *Dispersal Data and the Spread of Invading Organisms*, Ecology **77**, 2027–2042.

R.H. Lamberson, R. McKelvey, B.R. Noon and C. Voss [1992], *A Dynamic Analysis of Northern Spotted Owl Viability in a Fragmented Forest Landscape*, Conservation Biology **6**, 505–512.

J.F. Lynch and D.F. Whigham [1984], *Effects of Fragmentation on Breeding Bird Communities in Maryland, U.S.A.*, Biological Conservation **28**, 287–324.

H.J. Mader, C. Schell and P. Kornacker [1990], *Linear Barriers to Arthropod Movements in the Landscape*, Biological Conservation **54**, 209–222.

J.R. Malcolm [1994], *Edge Effects in Central Amazonian Forest Fragments*, Ecology **75**, 2438–2445.

D.J. Mattson and M.M. Reid [1991], *Conservation of the Yellowstone Grizzly Bear*, Conservation Biology **5**, 364–373.

J.D. Murray [1989], *Mathematical Biology*, Springer-Verlag, Berlin.

M. Neubert, M. Kot and M.A. Lewis [1995], *Dispersal and Pattern Formation in a Discrete Time Predator-Prey model*, Theoret. Pop. Biology **48**, 7–43.

W.D. Newmark [1985], *Legal and Biotic Boundaries of Western North American National Parks: A Problem of Congruence*, Biological Conservation **33**, 197–208.

W.D. Newmark [1991], *Tropical Forest Fragmentation and the Local Extinction of Understory Birds in the Eastern Usambara Mountains*, Tanzania, Conservation Biology **5**, 67–78.

A. Okubo [1980], *Diffusion and Ecological Problems: Mathematical Models*, Springer-Verlag, Berlin.

D.J. Oxley, M.D. Fenton and G.R. Carmondy [1974], *The Effects of Roads on Populations of Small Mammals*, J. Applied Ecology **11**, 51–59.

W. Reh and A. Seitz [1990], *The Influence of Land Use on the Genetic Structure of the Common Frog* Rana temporaria, Biological Conservation **54**, 239–249.

D.A. Saunders, R.J. Hobbs and C.R. Margules [1991], *Biological Consequences of Ecosystem Fragmentation: A Review*, Conservation Biology **5**, 18–32.

C.M. Schonewald-Cox and J.W. Bayless [1986], *The Boundary Model: A Geographical Analysis of Design and Conservation of Nature Reserves*, Biological Conservation **38**, 305–322.

M.L. Shaffer [1981], *Minimum Population Sizes for Species Conservation*, BioScience **31**, 131–134.

D. Simberloff [1986], *The Proximate Causes of Extinction*, in *Patterns and Processes in the History of Life* (D.M. Raup and D. Jablonski, eds.), Springer-Verlag, Berlin, 259–276.

J.A. Stamps, M. Buechner and V.V. Krishnan [1987], *The Effects of Edge-Permeability and Habitat Geometry on Emigration from Patches of Habitat*, The American Naturalist **129**, 533–552.

R.W. Van Kirk [1995], *Integrodifference Models of Biological Growth and Dispersal*, Ph.D. Thesis, University of Utah, Salt Lake City, UT.

R.W. Van Kirk and M.A. Lewis [1997], *Integrodifference Models for Persistence in Fragmented Habitats*, Bull. Math. Biology **59**, 107–137.

R.R. Veit and M.A. Lewis [1996], *Dispersal, Population Growth and the Allee Effect: Dynamics of the House Finch Invasion of Eastern North America*, American Naturalist **148**, 255–274.

J.F. Wegner and G. Merriam [1979], *Movements by Birds and Small Mammals between a Wood and Adjoining Farmland Habitats*, J. Applied Ecology **16**, 349–357.

D.S. Wilcove [1985], *Nest Predation in Forest Tracts and the Decline of Migratory Songbirds*, Ecology **66**, 1211–1214.

D.S. Wilcove and R.M. May [1986], *National Park Boundaries and Ecological Realities*, Nature **324**, 206–207.